

Dynamical scaling laws in the quantum q -state clock chain

Jia-Chen Tang,^{1,2} Wen-Long You,^{1,2} Myung-Joong Hwang,^{3,4} and Gaoyong Sun^{1,2,*}

¹*College of Science, Nanjing University of Aeronautics and Astronautics, Nanjing, 211106, China*

²*Key Laboratory of Aerospace Information Materials and Physics (Nanjing University of Aeronautics and Astronautics), MIIT, Nanjing 211106, China*

³*Division of Natural and Applied Sciences, Duke Kunshan University, Kunshan, Jiangsu 215300, China*

⁴*Zu Chongzhi Center for Mathematics and Computational Science, Duke Kunshan University, Kunshan, Jiangsu 215300, China*

We show that phase transitions in the quantum q -state clock model for $q \leq 4$ can be characterized by a decay enhanced behavior of the Loschmidt echo via a small quench. The quantum criticality of the quantum q -state clock model is numerically investigated by the finite-size scaling of the first minimum of the Loschmidt echo and the short-time average of rate function. The equilibrium correlation length critical exponents that are obtained from the scaling laws are consistent with previous results. More importantly, we study dynamical quantum phase transitions in the quantum q -state clock model by analyzing the Loschmidt echo and the order parameter for any q upon a big quench. For $q \leq 4$, we show that dynamical quantum phase transitions can be described by the Loschmidt echo and the zeros of the order parameter. In particular, we find the rate function increases logarithmically with q at the first critical time t_{c1} . However, for $q > 4$, we do not find a convincing evidence of a relationship between the Loschmidt echo and the zeros of the order parameter for dynamical quantum phase transitions. The Loschmidt echo near its first minimum seems to converge, while the order parameter at its first zero increases linearly with q .

I. INTRODUCTION

Continuous phase transitions in equilibrium are central concepts in quantum many-body systems¹. The nature of phase transitions can usually be demonstrated by the universality classes and the order parameters from the renormalization group^{2,3} and the finite-size scaling theory^{4,5}. Using the theoretical tools of quantum information science, quantum phase transitions and critical phenomena in equilibrium can also be understood by the quantum entanglement^{6–8}, the ground-state fidelity^{9–19} and the Loschmidt echo^{20–22}. In contrast to the quantum entanglement and the ground-state fidelity, the Loschmidt echo is much easier to be measured in experiment upon a sudden quench. Recently, the dynamical scaling laws of the Loschmidt echo are established to extract equilibrium critical exponents of many-body systems by the finite-size scaling theory for second-order phase transitions²¹. For instance, the universality class of phase transitions in one-dimensional Hermitian²¹ and non-Hermitian transverse field Ising chain²² were identified by the Loschmidt echoes.

On the other hand, the generation of equilibrium phase transitions to the nonequilibrium systems^{23,24} are attractive from the perspective of exploring unconventional phase transitions. Recently, an interesting nonequilibrium phase transition, named the dynamical quantum phase transition (DQPT)^{25–27}, is introduced to occur during the real-time evolution of a system upon a sudden quench. DQPTs that have attracted extensive attention often take place after a sudden large quench of the system across equilibrium quantum critical points in the thermodynamic limit^{25,28,29}, which was investigated in various systems subsequently^{30–38}. A dynamical quantum phase transitions is usually described by the Loschmidt echo²⁵,

where the rate function shows a nonanalyticity at critical times t_c . Moreover, a DQPT arising from the large quench is often characterized by the zeros of an order parameter^{25,28–30} at the critical time t_c . It is argued recently that the dynamics of such a DQPT is analogous to a two-level system dynamics³⁹. A key issue is whether the DQPT can exhibit a complex many-body dynamics or merely behave as a two-level system^{40–42}. Inspired by these, we investigate the quench dynamics in the quantum q -state clock model where the Loschmidt echoes can be analytically solved^{43,44} for some special quench protocols focusing on the following two issues: 1) whether the Loschmidt echo can be used to detect equilibrium second-order phase transitions when discrete symmetries are present. 2) What is the relationship between the Loschmidt echo and the zeros of an order parameter of the DQPT in the q -state clock model.

In this paper, we first use the Loschmidt echo to explore equilibrium second-order phase transitions in the q -state clock model and to identify the finite-size dynamical scaling and the correlation length critical exponents for $q \leq 4$. We find that the decay of the Loschmidt echo is enhanced near the equilibrium critical point, through which we obtain the equilibrium correlation length critical exponents. We show that in the absence of the knowledge of the critical point and the phase transition, one can use the short-time average rate function to study the quantum criticality even in the presence of discrete symmetries. In addition, we develop a more flexible and achievable method to perform the finite-size scaling for extracting equilibrium critical exponents by simply using the first minima of the Loschmidt echoes of a 3D plot.

Furthermore, we investigate the DQPTs of the q -state clock model upon a big quench for any q . We derive analytical solutions of both the Loschmidt echo and the order

parameter for arbitrary q , where we show that DQPTs denoted by the Loschmidt echo singularity can be connected to the zeros of the order parameters for $q \leq 4$. In particular, we find the value of the rate function of the Loschmidt echo of $q = 4$ is twice as much as that of $q = 2$. In addition, we show that the rate function increases logarithmically with q at the first critical time t_c in the regime $q \leq 4$. While, for $q > 4$, we find that the Loschmidt echo singularity does not correspond to the zeros of the order parameters. The Loschmidt echo at its first minimum converges, and the order parameter at its first zero increases linearly with q .

This paper is organized as follows. In Sec. II, we introduce the quantum q -state clock model. In Sec. III, we discuss the scaling law of the Loschmidt echo. In Sec. IV, we demonstrate the equilibrium quantum criticalities of the q -state clock model upon a small quench for $q \leq 4$. In Sec. V, we study the DQPTs of the q -state clock model upon a big quench for any q . In Sec. VI, we summarize our results.

II. Q-STATE CLOCK MODEL

We consider a general one-dimensional quantum q -state clock model of N sites with periodic boundary condition, whose Hamiltonian is given by^{45–48},

$$H = -J \sum_{j=1}^N (U_{j+1}^\dagger U_j + U_j^\dagger U_{j+1}) - h \sum_{j=1}^N (V_j + V_j^\dagger), \quad (1)$$

where the kinetic energy term is represented by the unitary operator U_j with the coupling coefficient J , the other unitary operator V_j denotes the potential energy term with the coupling constant h . The periodic boundary condition is imposed as $U_{N+1} = U_1$. We label the q states of the local Hilbert space at the site j by $|0\rangle_j, \dots, |m\rangle_j, \dots, |q\rangle_j$ with $0 < m < q$. In these orthogonal bases, the operators U_j and V_j are written as,

$$U_j = \begin{pmatrix} 1 & 0 & 0 & 0 & \dots & 0 \\ 0 & \omega & 0 & 0 & \dots & 0 \\ 0 & 0 & \omega^2 & \dots & 0 & \\ 0 & 0 & 0 & \omega^3 & \dots & 0 \\ \vdots & \vdots & \vdots & \vdots & \ddots & \vdots \\ 0 & 0 & 0 & 0 & \dots & \omega^{q-1} \end{pmatrix}, \quad (2)$$

$$V_j = \begin{pmatrix} 0 & 1 & 0 & 0 & \dots & 0 \\ 0 & 0 & 1 & 0 & \dots & 0 \\ 0 & 0 & 0 & 1 & \dots & 0 \\ \vdots & \vdots & \vdots & \vdots & \ddots & \vdots \\ 0 & 0 & 0 & 0 & \dots & 1 \\ 1 & 0 & 0 & 0 & \dots & 0 \end{pmatrix}. \quad (3)$$

Here, the unitary operator U_j is a diagonal matrix in which diagonal elements are ω^k with $\omega = e^{i2\pi/q} \equiv e^{i\theta}$

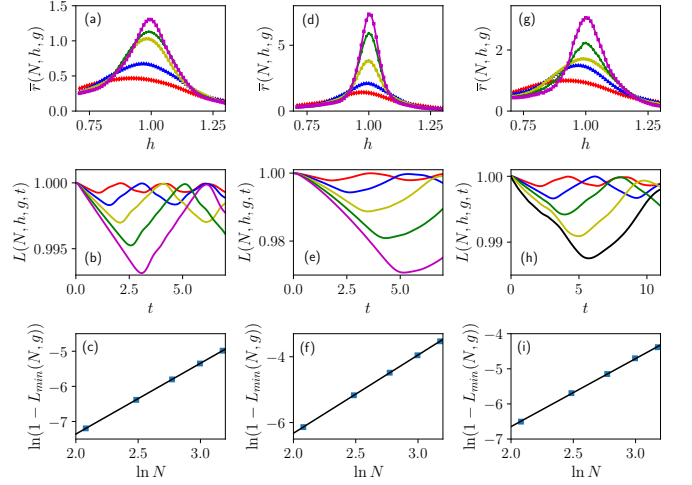


FIG. 1. Scaling of the short-time average rate function and the Loschmidt echo of the q -state clock model. (a) The short-time average rate function $\bar{r}(N, h, g)$ with respect to h with $g = 0.01$ in different lattice sizes $N = 8, 12, 16, 20, 24$ (from bottom to top along the peaks) for $q = 2$. (b) The Loschmidt echo $L(N, h, g, t)$ at the peak position h_* of $\bar{r}(N, h, g)$ in (a) with $g = 0.01$ as a function of time t for lattice sizes $N = 8, 12, 16, 20, 24$ (from top to bottom along the first minima). (c) Finite-size scaling of $1 - L_{\min}(N, g)$ obtained from (b) as a function of lattice sizes N , where the black square symbols are numerical values, the black solid line denotes the fitting curve. The correlation length critical exponent $\nu = 0.992$ is obtained from the fitting curve. Here (d), (e) and (f) represent the short-time average rate function, the Loschmidt echo and the finite-size scaling of $1 - L_{\min}(N, g)$ for $q = 3$, respectively. The corresponding data for $q = 4$ are shown in (g), (h) and (i), respectively. The correlation length critical exponents obtained from fitting curves are $\nu = 0.842$ for $q = 3$ and $\nu = 1.033$ for $q = 4$.

and $k = 0, 1, \dots, q - 1$ for arbitrary integers q . And U_j and V_j obey the following relations,

$$V_j U_j = \omega V_j U_j \quad (4)$$

$$U_j^q = V_j^q = 1 \quad (5)$$

The quantum q -state clock model undergoes second-order phase transitions^{45–48} for $q \leq 4$ and Berezinskii-Kosterlitz-Thouless (BKT) transitions for $q > 4$. In the following, we will study the q -state clock model out of equilibrium by considering the following two cases: One case is that we will discover equilibrium second-order phase transitions of $q \leq 4$ by the Loschmidt echo as well as its short-time average of rate function upon a small sudden quench. The other case is that we will investigate DQPTs by the Loschmidt echo and the order parameter upon a big sudden quench for any q .

III. SCALING LAWS OF LOSCHMIDT ECHO

Given an arbitrary initial state $|\psi_0\rangle$, the time evolution under a post-quenched time-independent Hamiltonian H_f is given by,

$$|\psi(t)\rangle = e^{-iH_f t}|\psi_0\rangle, \quad (6)$$

where \hbar is set as $\hbar = 1$. The Loschmidt echo is defined by the return probability (or time-evolved fidelity),

$$L(t) = |\langle\psi_0|e^{-iH_f t}|\psi_0\rangle|^2, \quad (7)$$

with the Loschmidt amplitude $G(t) = \langle\psi_0|\psi(t)\rangle$.

It has been shown that the decay of the Loschmidt echo can be enhanced by the equilibrium quantum criticality. The first minimum of the Loschmidt echo at the time $t_{min,1}$ is shown recently to scale as,

$$1 - L_{min}(N, g) \propto g^2 N^{2/\nu}, \quad (8)$$

at the equilibrium critical point for second-order phase transitions. Here g is the small constant step defined by,

$$g = h_f - h_i, \quad (9)$$

with h_i and h_f are two coupling constants of the clock model to control quench protocols. The dynamical scaling law in Eq.(8) that governs the critically enhanced decay behavior of the Loschmidt echo with respect to N can be used to extract the equilibrium correlation length critical exponent ν . We note that the Loschmidt echo $L_{min}(N, g)$ should be computed at or near the equilibrium critical point h_c for performing the scaling law in Eq.(8). In order to study a system without knowing the critical point h_c in advance, the short-time average of the rate function,

$$\bar{r}(N, h, g) = -\frac{1}{N} \frac{\ln(\bar{L}(N, h, g))}{g^2}, \quad (10)$$

is introduced analogous to the ground-state fidelity susceptibility to find the $L_{min}(N, g)$. Here $\bar{L}(N, h)$ is the short-time average of the Loschmidt echo within the time T defined by,

$$\bar{L}(N, h, g) = \frac{1}{T} \int_0^T L(N, h, g, t) dt. \quad (11)$$

We note that the time T for the average should exceed $t_{min,1}$ in order to cover the value of $L_{min}(N, g)$.

On the other hand, the rate function of the Loschmidt echo given by,

$$r(t) = -\frac{1}{N} \ln L(t) \quad (12)$$

can reveal singularities, also named Loschmidt echo singularities, at the critical time t_c upon a big sudden quench. The singularities of the rate function often indicate that a system undergoes DQPTs. In the following, we will also use the rate function in Eq.(12) to analyze the DQPTs.

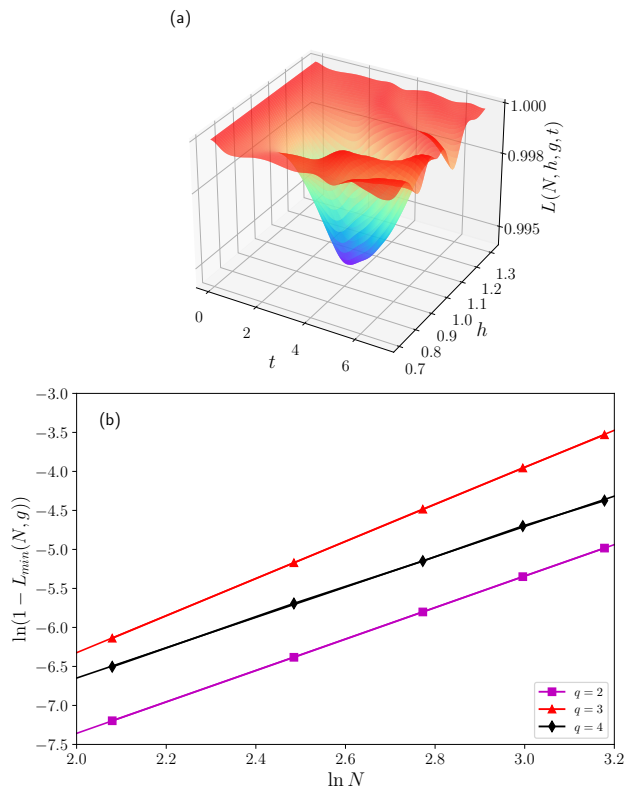


FIG. 2. Evolution and the scaling of the Loschmidt echo. (a) Time evolution of the Loschmidt echo $L(N, h, g, t)$ as the function of h and t for $q = 3$ with $g = 0.01$ in $N = 16$ lattice sites, which exhibits a decay behavior enhanced by the quantum criticality. (b) Finite-size scaling of the minima of the Loschmidt echoes $L_{min}(N, g)$ for $p = 2$ (purple square), $p = 3$ (red triangle), $p = 4$ (black diamond) with sizes $N = 8, 12, 16, 20, 24$. The correlation length critical exponents obtained from fitting curves are $\nu = 0.992$ for $q = 2$, $\nu = 0.842$ for $q = 3$ and $\nu = 1.029$ for $q = 4$.

IV. DYNAMICS UPON SMALL QUENCH

In the following, we will study the dynamics of the system upon a small quench. First of all, we obtain the ground-state $|\psi_0\rangle$ from Eq.(1) at the coupling h_i , then compute the Loschmidt echo from Eq.(7) by quenching the q -state clock model from the initial h_i to a final h_f with a small constant step $g = 0.01$. The time-evolved wave function $|\psi(t)\rangle$ is obtained from the time-dependent density matrix renormalization group (t-DMRG)^{49–53} with the step $\Delta t = 0.02$ under periodic boundary conditions, where we choose $J = 1$ during the numerical simulations. We will focus on the cases of $q \leq 4$ as the scaling law in Eq.(8) is argued to be valid for second-order phase transitions. The dynamical scaling laws of the Loschmidt echo are unknown for equilibrium BKT transitions to the best of our knowledge. Besides, the numerical simulations for $q > 4$ are difficult using the t-DMRG method with periodic boundary

conditions. The understanding of the scaling laws for equilibrium BKT transitions is left for future study.

We explain here how to use short-time average rate function to probe second-order phase transitions for $q \leq 4$ assuming that one knows nothing of the exact critical value in advance. We first calculate the corresponding short-time average rate functions $\bar{r}(N, h, g)$ from Eq.(10) by varying the coupling h and find the pseudo critical points h_* , which are derived from the peaks of short-time average rate functions for each lattice N as shown in Fig.1(a). We then perform numerical simulations upon a quench with the t-DMRG from this pseudo critical point h_* to $h_f = h_* + g$ for $N = 8, 12, 16, 20, 24$ sites. The results of the Loschmidt echoes $L(N, h, g, t)$ that are represented in Fig.1(b) exhibit a decay and revival dynamics. The first minimum of the Loschmidt echoes $L_{min}(N, g)$ are plotted in Fig.1(c) with respect to the lattice size N . According to the scaling law in Eq.(8), we obtain the critical exponent $\nu = 0.992$ for $q = 2$. Similarly, we find the critical exponent $\nu = 0.842$ when $q = 3$ and the critical exponent $\nu = 1.033$ when $q = 4$ as demonstrated in Fig.1 from (d) to (i).

The above results of the critical exponents are consistent with exact values, which are $\nu = 1$ for $p = 2, 4$ and $p = 5/6$ for $p = 3$. That is to say, the short-time average rate function is a validly flexible approach to probe phase transitions of the q -state clock model without knowing the critical value in advance. However, if we look carefully at the curves of short-time average rate functions for $p = 4$ shown in Fig.1(g), we can find that the curves are not smooth enough. Although it is not necessary to let the time T tends towards infinity, the choice of T may be highly confusing. In order to overcome this problem, we propose that the first minima in the 3D plot of the Loschmidt echoes [c.f Fig.(2)(a)] can serve as a probe to perform the finite-size scaling using the Eq.(8) to extract equilibrium critical exponents. The correlation length critical exponents obtained from first minima of the Loschmidt echoes $L_{min}(N, g)$ are $\nu = 0.992$ for $q = 2$, $\nu = 0.842$ for $q = 3$ and $\nu = 1.029$ for $q = 4$, respectively [c.f Fig.(2)(a)]. Interestingly, we derive a better correlation length critical exponent ν for $p = 4$ indicating that this simple method is more flexible and achievable.

V. DQPT UPON BIG QUENCH

Let us now consider the dynamics of the q -state clock model upon a big sudden quench. We first consider a special case by quenching the system from $h_i = \infty$ to $h_f = 0$, in which the rate function of the Loschmidt echo $r(t)$ often exhibits a singular behavior that can be characterized by the zeros of an order parameter. We derive analytic solutions of the Loschmidt echoes as well as the order parameters for any q . The corresponding results are discussed and divided into two parts: one part is the case when $q \leq 4$ and the other part is the case when $q > 4$.

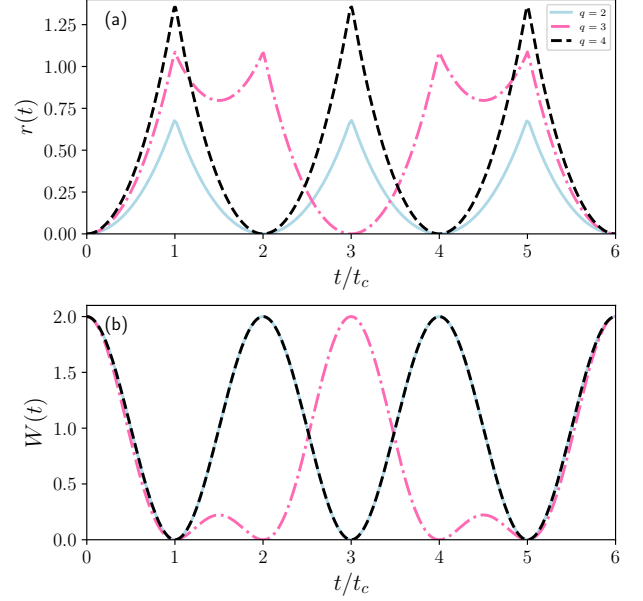


FIG. 3. Rate functions of Loschmidt echoes $r(t)$ and order parameters $W(t)$ upon a quench from $h_i = \infty$ to $h_f = 0$. (a) The rate function $r(t)$ as the function of t/t_c for $q \leq 4$ for $J = 1$ and $N = 100$ lattice sites, where the rate function $r(t)$ for $q = 4$ is twice the value of that for $q = 2$. Here, the first critical times t_c are $\pi/8$ for $q = 2$, $2\pi/9$ for $q = 3$ and $\pi/4$ for $q = 4$, respectively. (b) The order parameter $W(t)$ with respect to t_c with the same parameters as (a), whose zeros correspond to critical times h_c shown in (a).

The ground-state $|\psi_0\rangle$ of the q -state clock model at $h_i = \infty$ is the product state given by,

$$|\psi_0\rangle = \bigotimes_{j=1}^N |\phi\rangle_j \quad (13)$$

where, the local eigenstate $|\phi\rangle_j$ is,

$$|\phi\rangle_j = \left(\frac{1}{\sqrt{q}} \sum_{n=0}^{q-1} |n\rangle \right)_j = \frac{1}{\sqrt{q}} \begin{pmatrix} 1 \\ 1 \\ \vdots \\ 1 \\ 1 \end{pmatrix}. \quad (14)$$

The Loschmidt amplitude $G(t)$ in periodic boundary conditions can be simply written as,

$$G(t) = \text{tr} \mathbf{T}^N, \quad (15)$$

analogous to the partition function of the Ising model. Here T is a $q \times q$ matrix with the elements,

$$\mathbf{T}_{m_i, m_{i+1}} = \frac{1}{q} e^{iJt2 \cos(2\pi(m_{i+1} - m_i)/q)}, \quad (16)$$

and $m_i = 0, 1, \dots, q-1$. The Loschmidt amplitude can be

written as,

$$G(t) = \sum_{i=1}^q \Lambda_i^N, \quad (17)$$

as well in terms of the eigenvalues Λ_i of the matrix \mathbf{T} . Consequently, one can analytically investigate the behaviors of the Loschmidt echo, which we will go into details below.

Let us now introduce an order parameter defined by,

$$W(t) = \frac{1}{N} \langle \psi(t) | \sum_j (V_j + V_j^\dagger) | \psi(t) \rangle. \quad (18)$$

If the operator V_j is written in terms of the $\{|n\rangle\}$ as,

$$V_j = \sum_{n=0}^{q-1} |n\rangle \langle n+1|, \quad (19)$$

with a condition $|q\rangle \equiv |0\rangle$, the time-evolved order parameter $W(t)$ can be simply derived as (see Appendix A),

$$W(t) = \frac{1}{N} \langle \psi_0 | e^{-iJt \sum_i (U_{i+1}^\dagger U_i + U_i^\dagger U_{i+1})} \sum_j (V_j + V_j^\dagger) e^{iJt \sum_i (U_{i+1}^\dagger U_i + U_i^\dagger U_{i+1})} | \psi_0 \rangle \quad (20)$$

$$= \frac{1}{q^3} \sum_{m=0}^{q-1} \left(\sum_n e^{-4iJt \sin(\frac{\theta}{2}) \sin((m-n+\frac{1}{2})\theta)} \right)^2 + h.c., \quad (21)$$

in periodic boundary conditions. We will identify the DQPTs based on this analytic solution of the order parameter.

A. Dynamics for $q \leq 4$

Let us first consider the simplest case $q = 2$, for which the matrix \mathbf{T} ,

$$\mathbf{T} = \frac{1}{2} \begin{pmatrix} e^{2iJt} & e^{-2iJt} \\ e^{-2iJt} & e^{2iJt} \end{pmatrix}. \quad (22)$$

The corresponding two eigenvalues of \mathbf{T} are $\Lambda_1 = \frac{1}{2}e^{-2iJt}(e^{4iJt} - 1)$ and $\Lambda_2 = \frac{1}{2}e^{-2iJt}(e^{4iJt} + 1)$, therefore we have the Loschmidt amplitude,

$$G(t) = [\frac{1}{2}e^{-2iJt}(e^{4iJt} - 1)]^N + [\frac{1}{2}e^{-2iJt}(e^{4iJt} + 1)]^N. \quad (23)$$

The critical times for $q = 2$ are given by,

$$t_{cn} = \frac{\pi}{8J}(2n+1), \quad (24)$$

with $n \in \mathbb{N}$ by finding the zeros (or minima) of the Loschmidt echo $L(t) = |G(t)|^2$ depending on the finite

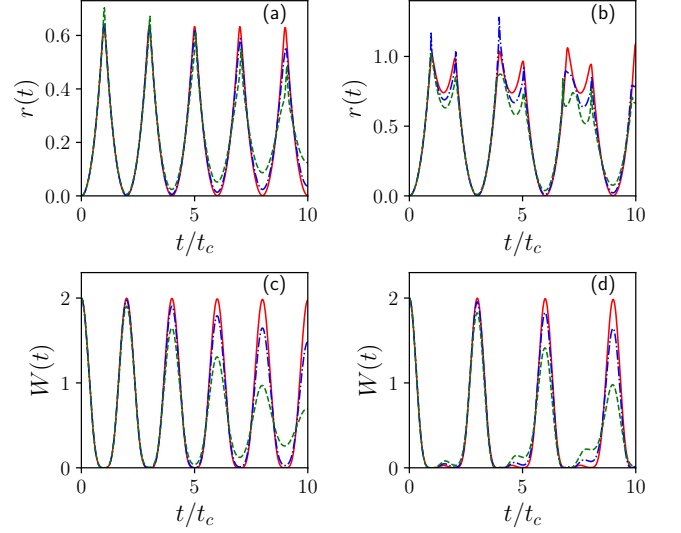


FIG. 4. Rate functions $r(t)$ and order parameters $W(t)$. The dynamics is obtained for $J = 1$ and $N = 24$ lattice sites by quenching the system from $h_i = \infty$ to $h_f = 0.01$ (red solid line), $h_f = 0.05$ (blue dashed-dot line) and $h_f = 0.1$ (green dashed line), respectively. (a) The rate functions $r(t)$ as the functions of t/t_c for $q = 2$, $t_c = \pi/8$. (c) The order parameters $W(t)$ as the functions of t/t_c for $q = 2$. The corresponding data for $q = 3$, $t_c = 2\pi/9$ are shown in (c) and (d), respectively

N . At the first critical point $t_{c1} = \frac{\pi}{8J}$, we obtain the rate function,

$$r(t_{c1}) = -\frac{1}{N} \ln L(t_{c1}) = \ln 2 - \frac{1}{N} \ln(1 + i^N)^2, \quad (25)$$

which becomes $\ln 2$ as the system size N tends to infinity. This result is interesting as the rate function $L(t)$ does not diverge but converge to a finite value $\ln 2$ in the thermodynamic limit.

Let us continue to investigate whether the rate function $L(t)$ has similar properties for $q = 3$. The matrix \mathbf{T} for $q = 3$ is given by,

$$\mathbf{T} = \frac{1}{3} \begin{pmatrix} e^{2iJt} & e^{-iJt} & e^{-iJt} \\ e^{-iJt} & e^{2iJt} & e^{-iJt} \\ e^{-iJt} & e^{-iJt} & e^{2iJt} \end{pmatrix}. \quad (26)$$

The eigenvalues of \mathbf{T} are $\Lambda_1 = \Lambda_2 = \frac{1}{3}e^{-iJt}(e^{3iJt} - 1)$ and $\Lambda_3 = \frac{1}{3}e^{-iJt}(e^{3iJt} + 2)$, respectively. We obtain the Loschmidt amplitude,

$$G(t) = 2[\frac{1}{3}e^{-iJt}(e^{3iJt} - 1)]^N + [\frac{1}{3}e^{-iJt}(e^{3iJt} + 2)]^N. \quad (27)$$

The critical times for $q = 3$ are given

$$t_{cn}^1 = \frac{2\pi}{9J}(3n+1), \quad (28)$$

$$t_{cn}^2 = \frac{2\pi}{9J}(3n+2). \quad (29)$$

The rate function is found to be $\ln 3$ at the first critical time $t_{c1} = t_{c1}^1 = \frac{2\pi}{9J}$ as the system size N tends to infinity as expected.

Let us continue. When $q = 4$, the matrix \mathbf{T} is,

$$\mathbf{T} = \frac{1}{4} \begin{pmatrix} e^{2iJt} & 1 & e^{-2iJt} & 1 \\ 1 & e^{2iJt} & 1 & e^{-2iJt} \\ e^{-2iJt} & 1 & e^{2iJt} & 1 \\ 1 & e^{-2iJt} & 1 & e^{2iJt} \end{pmatrix}. \quad (30)$$

The eigenvalues of \mathbf{T} are $\Lambda_1 = \frac{1}{4}e^{-2iJt}(e^{2iJt} - 1)^2$, $\Lambda_2 = \frac{1}{4}e^{-2iJt}(e^{2iJt} + 1)^2$, $\Lambda_3 = \Lambda_4 = \frac{1}{4}e^{-2iJt}(e^{4iJt} - 1)$. Therefore we have,

$$G(t) = \left[\frac{1}{4}e^{-2iJt}(e^{2iJt} - 1)^2\right]^N + \left[\frac{1}{4}e^{-2iJt}(e^{2iJt} + 1)^2\right]^N + 2\left[\frac{1}{4}e^{-2iJt}(e^{4iJt} - 1)\right]^N, \quad (31)$$

Similarly, the critical times for $q = 4$ are given by,

$$t_{cn} = \frac{\pi}{4J}(2n+1), \quad (32)$$

Interestingly, the rate function is found to be $\ln 4$ at the first critical time $t_{c1} = \frac{\pi}{4J}$ as the system size N tends to infinity (see Appendix B). As a consequence, we prove that the rate function increases logarithmically with q at the first critical time t_{c1} for $q \leq 4$ (c.f. Fig.3(a)). Moreover, analytical results show that the rate function $r(t)$ for $q = 4$ is twice as big as that of $q = 2$ (see Fig.3(a) and Appendix C).

We have studied the rate function of the Loschmidt echo in an arbitrary finite system N for $q \leq 4$. In the following, we will discuss the order parameter $W(t)$ of DQPTs, which is argued to zero at critical times that can be connected to the Loschmidt echo singularity for $q \leq 4$. When $q = 2$, the order parameter $W(t)$ is given by (see Appendix D),

$$W(t) = \frac{1}{2^3} \sum_m \left(\sum_n e^{-4iJt \sin(\frac{\pi}{2}) \sin((m-n+\frac{1}{2})\pi)} \right)^2 + h.c. = 2 \cos^2(4Jt). \quad (33)$$

In the same way, the order parameters $W(t)$ are equal to $\frac{2}{9}[(2 \cos(3Jt) + 1)^2]$ and $2 \cos^2(2Jt)$ for $q = 3$ and $q = 4$, respectively as shown in Fig.3(b), where we find a one-to-one relationship between the Loschmidt echo singularity and the zeros of the order parameter (see Appendix D).

In order to consider quantum fluctuations during the time evolution, we quench the system from $h_i = \infty$ to $h_f = 0.01$, $h_f = 0.05$ and $h_f = 0.1$. The corresponding

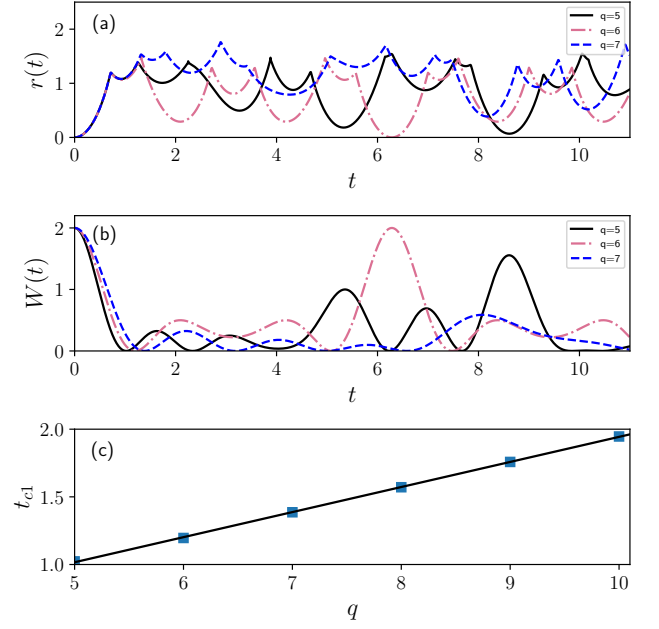


FIG. 5. Quench dynamics from $h_i = \infty$ to $h_f = 0$ for $q > 4$. (a) Rate functions $r(t)$ as the functions of t for $q = 5, 6, 7$ with $J = 1$ and $N = 100$ lattice sites, which tends to converge at the first cusp. (b) Order parameters $W(t)$ with the same parameters as (a). (c) The time t_{c1} obtained from the first zeros of order parameters $W(t)$ with respect to the q . The blue square symbols are numerical results, and the black solid line is the fitting curve.

Loschmidt echoes and order parameters are computed by using the t-DMRG method for $N = 24$ lattice sites in periodic boundary conditions. We find that DQPTs can survive in short time, where rate functions of the Loschmidt echoes $r(t)$ display the kinks, which can be characterized by the order parameters $W(t)$ as well compared to the case of $h_f = 0$ [c.f. Fig.4].

B. Dynamics for $q > 4$

We have shown our main results of DQPTs for $q \leq 4$. It is fascinating to study DQPTs upon a quench across a critical point with a different universality class. For example, an exact mapping of DQPTs can be established for a quench across the Ising model transition and a quench across a deconfined quantum critical point²⁹. In the following, we will present the results for $q > 4$ upon a quench across a BKT transition. The general results of the Loschmidt amplitude $G(t)$ in Eq.(17) and order parameters $W(t)$ in Eq.(21) are still valid for the cases $q > 4$. However, it is difficult to obtain the simple analytical formulas when $q > 4$. We will discuss the DQPTs based on the numerical results.

We find that the DQPTs persist for $q > 4$, where rate functions $r(t)$ exhibit non-analytical behaviors as-

sociated with linear cusps [c.f. Fig.5(a)]. Interestingly, the Loschmidt echo for $q > 4$ at the first critical time seems to converge instead of a logarithmical increase with q for $q < 4$. However, the zeros of order parameters cannot be connected to the Loschmidt echo singularity [c.f. Fig.5(b)], indicating the DQPTs for $q > 4$ are beyond two-level dynamics. In addition, we find that the critical times t_{c1} obtained from the first zeros of the order parameters $W(t)$ increase linearly with the q as shown in Fig.5(c) for $q > 4$. The understanding of these features is still incomplete, which we defer to future study.

VI. CONCLUSION

In summary, we have studied the finite-size dynamical scaling laws of the Loschmidt echo in the quantum q -state clock model. We have shown that the short-time average rate function and the first minimum of the Loschmidt echo in the 3D plot can serve as probes to detect equilibrium second-order phase transitions without knowing the accurate critical values in advance in the presence of discrete Z_p symmetry. The equilibrium correlation length critical exponents ν are obtained for $q \leq 4$ are consistent with previous results. It would be very interesting to establish dynamical scaling laws of the Loschmidt echo for BKT transitions to know whether the Loschmidt echo can characterize BKT transitions as the ground-state fidelity in the future.

We derive analytic results for the Loschmidt echo $L(t)$

and the order parameter $W(t)$ for any q , which have been used to understand DQPTs of the q -state clock model. For $q \leq 4$, we have shown that the Loschmidt echo singularity is connected to the zeros of the order parameter $W(t)$. In particular, the rate function is found to increase logarithmically with q at the critical times. While when $q > 4$, there is not a consistent one-to-one correspondence between the Loschmidt echo and the order parameter. The complete understanding of DQPTs upon a quench across a BKT transition is unknown, which is deferred to future study.

ACKNOWLEDGMENTS

G.S. was supported by the NSFC under the Grants No. 11704186 and No. 11874220. W.-L.Y. is appreciative of support from the NSFC under the Grant No. 12174194, the startup fund (Grant No. 1008-YAH20006) of Nanjing University of Aeronautics and Astronautics, Top-notch Academic Programs Project of Jiangsu Higher Education Institutions, and stable support for basic institute research (Grant No.190101). M.-J. H. was supported by NSFC under the Grant No. 12050410258, the Startup Fund from Duke Kunshan University, and Innovation Program for Quantum Science and Technology 2021ZD0301602. Numerical simulations were carried out on clusters of Nanjing University of Aeronautics and Astronautics.

-
- * Corresponding author: gysun@nuaa.edu.cn
- ¹ S. Sachdev, *Quantum Phase Transitions* (Cambridge University Press, Cambridge, 1999).
 - ² K. G. Wilson and J. Kogut, *Physics Reports* **12**, 75 (1974).
 - ³ K. G. Wilson, *Reviews of Modern Physics* **47**, 773 (1975).
 - ⁴ M. E. Fisher and M. N. Barber, *Physical Review Letters* **28**, 1516 (1972).
 - ⁵ M. E. Fisher, *Reviews of Modern Physics* **46**, 597 (1974).
 - ⁶ A. Osterloh, L. Amico, G. Falci, and R. Fazio, *Nature* **416**, 608 (2002).
 - ⁷ R. Horodecki, P. Horodecki, M. Horodecki, and K. Horodecki, *Reviews of Modern Physics* **81**, 865 (2009).
 - ⁸ J. Eisert, M. Cramer, and M. B. Plenio, *Reviews of Modern Physics* **82**, 277 (2010).
 - ⁹ W.-L. You, Y.-W. Li, and S.-J. Gu, *Physical Review E* **76**, 022101 (2007).
 - ¹⁰ L. Campos Venuti and P. Zanardi, *Physical Review Letters* **99**, 095701 (2007).
 - ¹¹ S. Chen, L. Wang, Y. Hao, and Y. Wang, *Physical Review A* **77**, 032111 (2008).
 - ¹² S.-J. Gu, H.-M. Kwok, W.-Q. Ning, and H.-Q. Lin, *Physical Review B* **77**, 245109 (2008).
 - ¹³ S. Yang, S.-J. Gu, C.-P. Sun, and H.-Q. Lin, *Physical Review A* **78**, 012304 (2008).
 - ¹⁴ S.-J. Gu, *International Journal of Modern Physics B* **24**, 4371 (2010).
 - ¹⁵ G. Sun, *Physical Review A* **96**, 043621 (2017).
 - ¹⁶ Z. Zhu, G. Sun, W.-L. You, and D.-N. Shi, *Physical Review A* **98**, 023607 (2018).
 - ¹⁷ Q. Luo, J. Zhao, and X. Wang, *Physical Review E* **98**, 022106 (2018).
 - ¹⁸ G. Sun, J.-C. Tang, and S.-P. Kou, *Frontiers of Physics* **17**, 1 (2022).
 - ¹⁹ Y.-N. Wang, W.-L. You, and G. Sun, *Physical Review A* **106**, 053315 (2022).
 - ²⁰ H. T. Quan, Z. Song, X. F. Liu, P. Zanardi, and C. P. Sun, *Physical Review Letters* **96**, 140604 (2006).
 - ²¹ M.-J. Hwang, B.-B. Wei, S. F. Huelga, and M. B. Plenio, *arXiv:1904.09937* (2019).
 - ²² J.-C. Tang, S.-P. Kou, and G. Sun, *Europhysics Letters* **137**, 40001 (2022).
 - ²³ G. Ódor, *Reviews of Modern Physics* **76**, 663 (2004).
 - ²⁴ H. Weimer, A. Kshetrimayum, and R. Orús, *Reviews of Modern Physics* **93**, 015008 (2021).
 - ²⁵ M. Heyl, A. Polkovnikov, and S. Kehrein, *Physical Review Letters* **110**, 135704 (2013).
 - ²⁶ M. Heyl, *Reports on Progress in Physics* **81**, 054001 (2018).
 - ²⁷ J. Marino, M. Eckstein, M. S. Foster, and A. M. Rey, *Reports on Progress in Physics* **85**, 116001 (2022).
 - ²⁸ I. Hagymási, C. Hubig, Ö. Legeza, and U. Schollwöck, *Physical Review Letters* **122**, 250601 (2019).
 - ²⁹ G. Sun and B.-B. Wei, *Physical Review B* **102**, 094302 (2020).

- (2020).
- ³⁰ P. Jurcevic, H. Shen, P. Hauke, C. Maier, T. Brydges, C. Hempel, B. P. Lanyon, M. Heyl, R. Blatt, and C. F. Roos, *Physical review letters* **119**, 080501 (2017).
- ³¹ N. Fläschner, D. Vogel, M. Tarnowski, B. Rem, D.-S. Lühmann, M. Heyl, J. Budich, L. Mathey, K. Sengstock, and C. Weitenberg, *Nature Physics* **14**, 265 (2018).
- ³² X.-Y. Xu, Q.-Q. Wang, M. Heyl, J. C. Budich, W.-W. Pan, Z. Chen, M. Jan, K. Sun, J.-S. Xu, Y.-J. Han, C.-F. Li, and G.-C. Guo, *Light: Science & Applications* **9**, 1 (2020).
- ³³ K. Wang, X. Qiu, L. Xiao, X. Zhan, Z. Bian, W. Yi, and P. Xue, *Physical review letters* **122**, 020501 (2019).
- ³⁴ T. Tian, Y. Ke, L. Zhang, S. Lin, Z. Shi, P. Huang, C. Lee, and J. Du, *Physical Review B* **100**, 024310 (2019).
- ³⁵ X.-Y. Guo, C. Yang, Y. Zeng, Y. Peng, H.-K. Li, H. Deng, Y.-R. Jin, S. Chen, D. Zheng, and H. Fan, *Physical Review Applied* **11**, 044080 (2019).
- ³⁶ X. Nie, B.-B. Wei, X. Chen, Z. Zhang, X. Zhao, C. Qiu, Y. Tian, Y. Ji, T. Xin, D. Lu, and J. Li, *Physical Review Letters* **124**, 250601 (2020).
- ³⁷ T. Tian, H.-X. Yang, L.-Y. Qiu, H.-Y. Liang, Y.-B. Yang, Y. Xu, and L.-M. Duan, *Physical Review Letters* **124**, 043001 (2020).
- ³⁸ L.-N. Wu, J. Nettersheim, J. Feß, A. Schnell, S. Burgardt, S. Hiebel, D. Adam, A. Eckardt, and A. Widera, *arXiv:2208.05164* (2022).
- ³⁹ J. Zakrzewski, *arXiv:2204.09454* (2022).
- ⁴⁰ M. Van Damme, J.-Y. Desaulles, Z. Papić, and J. C. Halimeh, *arXiv:2210.02453* (2022).
- ⁴¹ Á. L. Corps and A. Relaño, *arXiv:2205.03443* (2022).
- ⁴² O. Kuliashov, A. Markov, and A. Rubtsov, *arXiv:2211.14256* (2022).
- ⁴³ C. Karrasch and D. Schuricht, *Physical Review B* **95**, 075143 (2017).
- ⁴⁴ Y. Wu, *Physical Review B* **101**, 014305 (2020).
- ⁴⁵ H. Matsuo and K. Nomura, *Journal of Physics A: Mathematical and General* **39**, 2953 (2006).
- ⁴⁶ G. Ortiz, E. Cobanera, and Z. Nussinov, *Nuclear Physics B* **854**, 780 (2012).
- ⁴⁷ J. Chen, H.-J. Liao, H.-D. Xie, X.-J. Han, R.-Z. Huang, S. Cheng, Z.-C. Wei, Z.-Y. Xie, and T. Xiang, *Chinese Physics Letters* **34**, 050503 (2017).
- ⁴⁸ G. Sun, T. Vekua, E. Cobanera, and G. Ortiz, *Physical Review B* **100**, 094428 (2019).
- ⁴⁹ U. Schollwöck, *Annals of Physics* **326**, 96 (2011).
- ⁵⁰ R. Orús, *Annals of physics* **349**, 117 (2014).
- ⁵¹ A. J. Daley, C. Kollath, U. Schollwöck, and G. Vidal, *Journal of Statistical Mechanics: Theory and Experiment* **2004**, P04005 (2004).
- ⁵² G. Vidal, *Physical review letters* **93**, 040502 (2004).
- ⁵³ G. Vidal, *Physical review letters* **98**, 070201 (2007).

Appendix A: Derivation of order parameters

In this section, we will show the details of the derivation of the order parameter $W(t)$, which is defined by,

$$W(t) = \langle V(t) + V^\dagger(t) \rangle \quad (A1)$$

$$= \frac{1}{N} \sum_j \langle \Psi_0 | (V_j + V_j^\dagger) | \Psi_0 \rangle \quad (A2)$$

$$= \langle \Psi_0 | e^{-iJt \sum_i (U_{i+1}^\dagger U_i + U_i^\dagger U_{i+1})} (V_1 + V_1^\dagger) e^{iJt \sum_i (U_{i+1}^\dagger U_i + U_i^\dagger U_{i+1})} | \Psi_0 \rangle \quad (A3)$$

$$= \langle \Psi_0 | e^{-iJt[(U_2^\dagger + U_N^\dagger)U_1 + U_1^\dagger(U_2 + U_N)]} (V_1 + V_1^\dagger) e^{iJt[(U_2^\dagger + U_N^\dagger)U_1 + U_1^\dagger(U_2 + U_N)]} | \Psi_0 \rangle \quad (A4)$$

Remember the operator V_j is,

$$V_j = \sum_{m=0}^{q-1} (|m\rangle \langle m+1|). \quad (A5)$$

we have,

$$W(t) = \langle \Psi_0 | e^{-iJt[(U_2^\dagger + U_N^\dagger)U_1 + U_1^\dagger(U_2 + U_N)]} \sum_{m=0}^{q-1} (|m\rangle \langle m+1|)_1 e^{iJt[(U_2^\dagger + U_N^\dagger)U_1 + U_1^\dagger(U_2 + U_N)]} | \Psi_0 \rangle + h.c., \quad (A6)$$

$$= \sum_{m=0}^{q-1} \langle \Psi_0 | e^{-iJt[e^{im\theta}(U_2^\dagger + U_N^\dagger) + e^{-im\theta}(U_2 + U_N)]} (|m\rangle \langle m+1|)_1 e^{iJt[e^{i(m+1)\theta}(U_2^\dagger + U_N^\dagger) + e^{-i(m+1)\theta}(U_2 + U_N)]} | \Psi_0 \rangle + h.c., \quad (A7)$$

$$= \sum_{m=0}^{q-1} \langle \Psi_0 | e^{iJt[(e^{i(m+1)\theta} - e^{im\theta})(U_2^\dagger + U_N^\dagger) + (e^{-i(m+1)\theta} - e^{-im\theta})(U_2 + U_N)]} (|m\rangle \langle m+1|)_1 | \Psi_0 \rangle + h.c. \quad (A8)$$

Because,

$$|\Psi_0\rangle = \bigotimes_{j=1}^N \left(\frac{1}{\sqrt{q}} \sum_n |n\rangle \right)_j \quad (A9)$$

and,

$$\langle m | \frac{1}{\sqrt{q}} \sum_n |n\rangle = \frac{1}{\sqrt{q}} \quad (\text{A10})$$

We have,

$$W(t) = \frac{1}{q} \sum_{m=0}^{q-1} \langle \Psi_0 | e^{iJt[(e^{i(m+1)\theta} - e^{im\theta})U_2^\dagger + (e^{-i(m+1)\theta} - e^{-im\theta})U_2]} e^{iJt[(e^{i(m+1)\theta} - e^{im\theta})U_N^\dagger + (e^{-i(m+1)\theta} - e^{-im\theta})U_N]} | \Psi_0 \rangle + h.c \quad (\text{A11})$$

$$= \frac{1}{q} \sum_{m=0}^{q-1} \left(\frac{1}{q} \sum_{n,n',n''} {}_2\langle n | e^{iJt[(e^{i(m+1)\theta} - e^{im\theta})U_2^\dagger]} (|n'\rangle\langle n'|) {}_2e^{iJt[(e^{-i(m+1)\theta} - e^{-im\theta})U_2]} |n''\rangle_2 \right)^2 + h.c \quad (\text{A12})$$

$$= \frac{1}{q} \sum_{m=0}^{q-1} \frac{1}{q^2} \left(\sum_n e^{iJt[(e^{i(m+1)\theta} - e^{im\theta})e^{-in\theta}]e^{iJt[(e^{-i(m+1)\theta} - e^{-im\theta})e^{in\theta}]} \right)^2 + h.c \quad (\text{A13})$$

$$= \frac{1}{q^3} \sum_{m=0}^{q-1} \left(\sum_n e^{iJt[(e^{i\theta} - 1)e^{i(m-n)\theta} + (e^{-i\theta} - 1)e^{i(n-m)\theta}]} \right)^2 + h.c \quad (\text{A14})$$

$$= \frac{1}{q^3} \sum_{m=0}^{q-1} \left(\sum_n e^{iJt[\frac{i\theta}{2}(e^{\frac{i\theta}{2}} - e^{-\frac{i\theta}{2}})e^{i(m-n)\theta} + e^{-\frac{i\theta}{2}}(e^{-\frac{i\theta}{2}} - e^{\frac{i\theta}{2}})e^{i(n-m)\theta}]} \right)^2 + h.c \quad (\text{A15})$$

$$= \frac{1}{q^3} \sum_{m=0}^{q-1} \left(\sum_n e^{iJt[(\frac{i\theta}{2} - e^{-\frac{i\theta}{2}})(e^{(m-n+\frac{1}{2})i\theta} - e^{-(m-n+\frac{1}{2})i\theta}]} \right)^2 + h.c \quad (\text{A16})$$

$$= \frac{1}{q^3} \sum_{m=0}^{q-1} \left(\sum_n e^{iJt[2i \sin(\frac{\theta}{2}) \cdot 2i \sin((m-n+\frac{1}{2})\theta)]} \right)^2 + h.c \quad (\text{A17})$$

$$= \frac{1}{q^3} \sum_{m=0}^{q-1} \left(\sum_n e^{-4iJt \sin(\frac{\theta}{2}) \sin((m-n+\frac{1}{2})\theta)} \right)^2 + h.c \quad (\text{A18})$$

We arrive at the general analytic solution of the order parameter $W(t)$.

Appendix B: Derivation of the rate function at first critical times

In this section, we present the details for the rate function at the first critical time t_c . When $q = 2$, Loschmidt amplitude $G(t)$ is

$$G(t) = \left(\frac{1}{2}e^{-2iJt}(e^{4iJt} - 1)\right)^N + \left(\frac{1}{2}e^{-2iJt}(e^{4iJt} + 1)\right)^N. \quad (\text{B1})$$

Place the first critical time $t = t_{c1} = \frac{\pi}{8J}$ into it, we have,

$$G(t) = 2^{-\frac{N}{2}}(1 + i^N). \quad (\text{B2})$$

The rate function $L(t)$ is written by,

$$r(t) = -\frac{1}{N} \ln L(t), \quad (\text{B3})$$

$$= \ln 2 - \frac{1}{N} \ln |1 + i^N|^2. \quad (\text{B4})$$

If the size of the system N tends to infinity, the rate function turns into $\ln 2$.

When $q = 3$, The matrix \mathbf{T} is,

$$\mathbf{T} = \frac{1}{3} \begin{pmatrix} e^{2iJt} & e^{-iJt} & e^{-iJt} \\ e^{-iJt} & e^{2iJt} & e^{-iJt} \\ e^{-iJt} & e^{-iJt} & e^{2iJt} \end{pmatrix} \quad (\text{B5})$$

The eigenvalues of \mathbf{T} are $\Lambda_1 = \Lambda_2 = \frac{1}{3}e^{-iJt}(e^{3iJt} - 1)$ and $\frac{1}{3}e^{-iJt}(e^{3iJt} + 2)$, respectively. Therefore we have,

$$G(t) = 2[\frac{1}{3}e^{-iJt}(e^{3iJt} - 1)]^N + [\frac{1}{3}e^{-iJt}(e^{3iJt} + 2)]^N \quad (\text{B6})$$

When placing the first critical time $t = t_c = \frac{2\pi}{9J}$ into $G(t)$, we have the following simple form,

$$G(t) = 3^{-N}e^{-i2N\pi/9}[2(e^{3iJt} - 1)^N + (e^{3iJt} + 2)^N] \quad (\text{B7})$$

Then the rate function is given by,

$$\begin{aligned} r(t) &= -\frac{1}{N} \ln L(t) \\ &= 2 \ln 3 - 1/N \ln |(9 \cos^2(3Jt/2) + \sin^2(3Jt/2))^N + 4^{N+1} \sin^{2N}(3Jt/2) \\ &\quad + 2(2i)^N (3 \cos(3Jt/2) + i \sin(3Jt/2))^N \sin^N(3Jt/2) \\ &\quad + 2(2i)^N (-3 \cos(3Jt/2) + i \sin(3Jt/2))^N \sin^N(3Jt/2)| \end{aligned} \quad (\text{B8})$$

It is not difficult to see if the size of the system N verge to infinity, the rate function turn into $\ln 3$.

Similarly, the matrix \mathbf{T} for $q = 4$ is,

$$\mathbf{T} = \frac{1}{4} \begin{pmatrix} e^{2iJt} & 1 & e^{-2iJt} & 1 \\ 1 & e^{2iJt} & 1 & e^{-2iJt} \\ e^{-2iJt} & 1 & e^{2iJt} & 1 \\ 1 & e^{-2iJt} & 1 & e^{2iJt} \end{pmatrix} \quad (\text{B10})$$

The eigenvalues of \mathbf{T} are $\Lambda_1 = \frac{1}{4J}e^{-2iJt}(e^{2iJt} - 1)^2$, $\Lambda_2 = \frac{1}{4}e^{-2iJt}(e^{2iJt} + 1)^2$, $\Lambda_3 = \Lambda_4 = \frac{1}{4}e^{-2iJt}(e^{4iJt} - 1)$. Therefore we have,

$$G(t) = [\frac{1}{4}e^{-2iJt}(e^{2iJt} - 1)^2]^N + [\frac{1}{4}e^{-2iJt}(e^{2iJt} + 1)^2]^N + 2[\frac{1}{4}e^{-2iJt}(e^{4iJt} - 1)]^N \quad (\text{B11})$$

When the critical time $t = t_{c1} = \frac{\pi}{4}$ is placed into $G(t)$, we have,

$$G(t) = 2^{-N}[1 + (-1)^N + 2i^N] \quad (\text{B12})$$

Then the rate function for $q = 4$ is obtained by,

$$r(t) = -\frac{1}{N} \ln L(t) \quad (\text{B13})$$

$$= \ln 4 - \frac{1}{N} \ln |1 + (-1)^N + 2i^N|^2 \quad (\text{B14})$$

Obviously, If the size of the system N tends to infinity, the rate function turn into $\ln 4$.

Appendix C: Relationship of rate functions for $q = 2$ and $q = 4$

In the section, we will go into detail about the relationship between the rate function of $q = 2$ and $q = 4$. We prove that the rate function $r(t)$ for $q = 4$ is twice as much as that of $q = 2$. For $q = 2$, we have the Loschmidt amplitude,

$$G(t) = [i \sin 2Jt]^N + [\cos 2Jt]^N \quad (\text{C1})$$

As there are four cases based on i^N , $G(t)$ have four forms,

$$G(t) = i(\sin 2Jt)^N + (\cos 2Jt)^N, \quad (N = 4n + 1) \quad (\text{C2})$$

$$G(t) = -(\sin 2Jt)^N + (\cos 2Jt)^N, \quad (N = 4n + 2) \quad (\text{C3})$$

$$G(t) = -i(\sin 2Jt)^N + (\cos 2Jt)^N, \quad (N = 4n + 3) \quad (\text{C4})$$

$$G(t) = (\sin 2Jt)^N + (\cos 2Jt)^N, \quad (N = 4n) \quad (\text{C5})$$

The Loschmidt echo have the following forms:

$$L(t) = (\sin 2Jt)^{2N} + (\cos 2Jt)^{2N}, \quad (N = 4n + 1) \quad (C6)$$

$$L(t) = [(\sin 2Jt)^N - (\cos 2Jt)^N]^2, \quad (N = 4n + 2) \quad (C7)$$

$$L(t) = (\sin 2Jt)^{2N} + (\cos 2Jt)^{2N}, \quad (N = 4n + 3) \quad (C8)$$

$$L(t) = [(\sin 2Jt)^N + (\cos 2Jt)^N]^2, \quad (N = 4n) \quad (C9)$$

For $q = 4$, as $\Lambda_1 = -\sin^2 Jt$, $\Lambda_2 = \cos^2 Jt$, $\Lambda_2 = \Lambda_3 = \frac{i}{2} \sin 2Jt$, we have the Loschmidt amplitude,

$$G(t) = [-\sin^2 Jt]^N + [\cos^2 Jt]^N + 2[\frac{i}{2} \sin 2Jt]^N, \quad (C10)$$

which has the following form,

$$G(t) = [-\sin^2 Jt]^N + [\cos^2 Jt]^N + 2i[\frac{1}{2} \sin 2Jt]^N \quad (N = 4n + 1) \quad (C11)$$

$$G(t) = [-\sin^2 Jt]^N + [\cos^2 Jt]^N - 2[\frac{1}{2} \sin 2Jt]^N \quad (N = 4n + 2) \quad (C12)$$

$$G(t) = [-\sin^2 Jt]^N + [\cos^2 Jt]^N - 2i[\frac{1}{2} \sin 2Jt]^N \quad (N = 4n + 3) \quad (C13)$$

$$G(t) = [-\sin^2 Jt]^N + [\cos^2 Jt]^N + 2[\frac{1}{2} \sin 2Jt]^N \quad (N = 4n) \quad (C14)$$

Consequently, the Loschmidt echo have the following forms:

When $N = 4n + 1$, it is,

$$L(t) = [(-\sin^2 Jt)^N + (\cos^2 Jt)^N + 2i(\frac{1}{2} \sin 2Jt)^N] \cdot [(-\sin^2 Jt)^N + (\cos^2 Jt)^N - 2i(\frac{1}{2} \sin 2Jt)^N] \quad (C15)$$

$$= (\sin Jt)^{4N} + 2(\sin Jt \cos Jt)^{2N} + (\cos Jt)^{4N} \quad (C16)$$

$$= [(\sin Jt)^{2N} + (\cos Jt)^{2N}]^2 \quad (C17)$$

When $N = 4n + 2$, it is,

$$L(t) = [(-\sin^2 Jt)^N + (\cos^2 Jt)^N - 2(\frac{1}{2} \sin 2Jt)^N] \cdot [(-\sin^2 Jt)^N + (\cos^2 Jt)^N - 2(\frac{1}{2} \sin 2Jt)^N] \quad (C18)$$

$$= [(\sin^2 Jt)^N + (\cos^2 Jt)^N - 2(\frac{1}{2} \sin 2Jt)^N] \cdot [(\sin^2 Jt)^N + (\cos^2 Jt)^N - 2(\frac{1}{2} \sin 2Jt)^N] \quad (C19)$$

$$= (\sin Jt)^{4N} + 2(\sin Jt \cos Jt)^{2N} + (\cos Jt)^{4N} - 4(\frac{1}{2} \sin^2 Jt \sin 2Jt)^N - 4(\frac{1}{2} \cos^2 Jt \sin 2Jt)^N + 4(\sin t \cos t)^{2N} \quad (C20)$$

$$= [(\sin Jt)^{2N} + (\cos Jt)^{2N}]^2 - 4(\sin Jt \cos Jt)^N [(\sin Jt)^{2N} + (\cos Jt)^{2N}] + 4(\sin t \cos t)^{2N} \quad (C21)$$

$$= [(\sin Jt)^{2N} - 2(\sin t \cos t)^N + (\cos Jt)^{2N}]^2 \quad (C22)$$

$$= [(\sin Jt)^N - (\cos Jt)^N]^4 \quad (C23)$$

When $N = 4n + 3$, it is,

$$L(t) = [(-\sin^2 Jt)^N + (\cos^2 Jt)^N - 2i(\frac{1}{2} \sin 2Jt)^N] \cdot [(-\sin^2 Jt)^N + (\cos^2 Jt)^N + 2i(\frac{1}{2} \sin 2Jt)^N] \quad (C24)$$

$$= (\sin Jt)^{4N} + 2(\sin Jt \cos Jt)^{2N} + (\cos Jt)^{4N} \quad (C25)$$

$$= [(\sin Jt)^{2N} + (\cos Jt)^{2N}]^2 \quad (C26)$$

When $N = 4n$, it is,

$$L(t) = [(-\sin^2 Jt)^N + (\cos^2 Jt)^N + 2(\frac{1}{2} \sin 2Jt)^N] \cdot [(-\sin^2 Jt)^N + (\cos^2 Jt)^N + 2(\frac{1}{2} \sin 2Jt)^N] \quad (C27)$$

$$= [(\sin^2 Jt)^N + (\cos^2 Jt)^N + 2(\frac{1}{2} \sin 2Jt)^N] \cdot [(\sin^2 Jt)^N + (\cos^2 Jt)^N + 2(\frac{1}{2} \sin 2Jt)^N] \quad (C28)$$

$$= [(\sin Jt)^{2N} + 2(\sin t \cos t)^N + (\cos Jt)^{2N}]^2 \quad (C29)$$

$$= [(\sin Jt)^N + (\cos Jt)^N]^4 \quad (C30)$$

Remember the critical times are $t_{cn} = \frac{\pi}{8J}(2n+1)$ and $t_{cn} = \frac{\pi}{4J}(2n+1)$ for $q=2$ and $q=4$. It is easy to find that the Loschmidt echo for $q=4$ is merely the square of the Loschmidt echo for $q=2$ as the function of t/t_{c1} . In other words, the rate function of the Loschmidt echo for $q=4$ are twice as big as that for $q=2$.

Appendix D: The order parameters of $q=2$ and $q=4$

When $q=2$, $\theta = \frac{2\pi}{2} = \pi$, we can obtain the order parameter:

$$W(t) = \langle V(t) + V^\dagger(t) \rangle \quad (D1)$$

$$= \frac{1}{2^3} \sum_{m=0}^1 \left(\sum_n e^{-4iJt \sin(\frac{\pi}{2}) \sin((m-n+\frac{1}{2})\pi)} \right)^2 + h.c \quad (D2)$$

$$= \frac{1}{8} \sum_{m=0}^1 (e^{-4iJt \sin(\frac{\pi}{2}) \sin((m+\frac{1}{2})\pi)} + e^{-4iJt \sin(\frac{\pi}{2}) \sin((m-\frac{1}{2})\pi)})^2 + h.c \quad (D3)$$

$$= 2 \times \frac{1}{8} (e^{-4iJt} + e^{-4iJt})^2 + h.c \quad (D4)$$

$$= \cos^2(4Jt) + h.c \quad (D5)$$

$$= 2 \cos^2(4Jt) \quad (D6)$$

When $q=3$, $\theta = \frac{2\pi}{3}$, the order parameter $W(t)$ is,

$$W(t) = \langle V(t) + V^\dagger(t) \rangle \quad (D7)$$

$$= \frac{1}{3^3} \sum_{m=0}^2 \left(\sum_n e^{-4iJt \sin(\frac{\pi}{3}) \sin((m-n+\frac{1}{2})\frac{2\pi}{3})} \right)^2 + h.c \quad (D8)$$

$$= \frac{1}{27} \sum_{m=0}^2 (e^{-4iJt \sin(\frac{\pi}{3}) \sin((m+\frac{1}{2})\frac{2\pi}{3})} + e^{-4iJt \sin(\frac{\pi}{3}) \sin((m-\frac{1}{2})\frac{2\pi}{3})} + e^{-4iJt \sin(\frac{\pi}{3}) \sin((m-\frac{3}{2})\frac{2\pi}{3})})^2 + h.c \quad (D9)$$

$$= \frac{1}{27} [3(e^{-3iJt} + e^{3iJt} + 1)^2] + h.c \quad (D10)$$

$$= \frac{2}{9} [(2 \cos(3Jt) + 1)^2] \quad (D11)$$

When $q=4$, $\theta = \frac{2\pi}{4} = \frac{\pi}{2}$, the order parameter W is equal to $2 \cos(2Jt)^2$.

$$W(t) = \langle V(t) + V^\dagger(t) \rangle \quad (D12)$$

$$= \frac{1}{4^3} \sum_{m=0}^3 \left(\sum_n e^{-4iJt \sin(\frac{\pi}{4}) \sin((m-n+\frac{1}{2})\frac{\pi}{2})} \right)^2 + h.c \quad (D13)$$

$$= \frac{1}{64} \sum_{m=0}^3 (e^{-4iJt \sin(\frac{\pi}{4}) \sin((m+\frac{1}{2})\frac{\pi}{2})} + e^{-4iJt \sin(\frac{\pi}{4}) \sin((m-\frac{1}{2})\frac{\pi}{2})} + e^{-4iJt \sin(\frac{\pi}{4}) \sin((m-\frac{3}{2})\frac{\pi}{2})} + e^{-4iJt \sin(\frac{\pi}{4}) \sin((m-\frac{5}{2})\frac{\pi}{2})})^2 + h.c \quad (D14)$$

$$= \frac{1}{64} [4(e^{-2iJt} + e^{2iJt} + e^{2iJt} + e^{-2iJt})^2] + h.c \quad (D15)$$

$$= \frac{1}{64} [4(4 \cos(2Jt))^2] + h.c \quad (D16)$$

$$= 2 \cos^2(2Jt) \quad (D17)$$